41. PETROGRAPHY OF BARREMIAN SYNRIFT SEDIMENTS, SITE 549, GOBAN SPUR[1]

Jim Mazzullo, Elsa K. Mazzullo, and Kim Henke, Department of Geology, Texas A & M University[2]

ABSTRACT

During Leg 80 of the Deep Sea Drilling Project, a 290-m section of calcareous and noncalcareous Barremian synrift sediments was drilled in Hole 549. A petrographic study of samples from this section was undertaken in an attempt to determine the general conditions under which these sediments accumulated.

The deposition of the Barremian synrift sediments apparently occurred in relatively shallow, semirestricted to open-marine environments during a marine transgression. The basal unit (Unit 10) consists of fine-grained terrigenous and calcareous debris deposited in very shallow nearshore waters, possibly in a lagoon, bay, or protected shelf area. The unit above (Unit 9), characterized by milliporoid boundstone and skeletal grains, represents sedimentation at a high-energy, well-oxygenated shelf margin. The uppermost unit, consisting of fossiliferous wackestone grading upward to nonfossiliferous micritic mudstone, represents relatively deep-water sedimentation in foreslope environments seaward of the shelf margin.

INTRODUCTION

During Leg 80 of the Deep Sea Drilling Project, a thin (290.65-m) section of calcareous and noncalcareous Barremian synrift sediments overlying a basement high was drilled in Hole 549. This section was subdivided into four lithologic units and various subunits on the basis of the shipboard description of lithology and sedimentary structures, and from these data a general model for the deposition of the sequence was formulated.

This paper reports an additional, more detailed study of samples from this same section. It serves to supplement our shipboard descriptions of the units and subunits with thin-section, X-ray, and scanning electron microscopy (SEM) data and to refine our model for the origin of the section. It also serves to evaluate the accuracy of smear-slide data generated on board ship in the description of sedimentary rocks.

This study is based on the analysis of 21 samples taken by a member of the scientific staff of Leg 80 (J. M.) during the cruise. These samples were carefully chosen to represent all the major lithologic types and units or subunits described in the synrift section by the scientific staff of that leg.

PETROGRAPHY OF BARREMIAN SYNRIFT SEDIMENTS

The Barremian synrift sediments in Hole 549 are divided into units and subunits on the basis of onboard descriptions of lithology and sedimentary structures. For ease of comparison with the site chapter (this volume), we consider each of these unit or subunits, and our samples from each, separately. We note at the start that our analyses of the sediments support the breakdown of the synrift section made by the scientific staff.

In the laboratory, each sample was split into three pieces: one piece was impregnated with resin and ground into a thin section from which textural and compositional data were gathered. A second piece was used to prepare an oriented mount for X-ray determination of the clay suite, and a third piece was mounted on an aluminum plug, coated with a gold-palladium alloy, and examined with a JSM-25S SEM to determine clay morphology.

Unit 8

This unit (673.85–755 m BSF) is a thick, upward-fining section of gray interbedded calcareous mudstones and sandy calcareous mudstones overlain by a thin unit of variegated calcareous mudstone.

Two samples from the sandy calcareous mudstone lithology (60-6, 76–78 cm and 61-3, 30–32 cm) were examined (Fig. 1). The sand content is high in these samples: 45 and 41%, respectively. It consists of bioclastic debris (22 and 19.5%, respectively), which specifically include recrystallized bivalve fragments (8 and 9.5%), echinoderms (5 and 7%), foraminifers (1 and 6%), brachiopods (<2%), molluscs (0 and 1.5%), and ostracods (<1%); as well as quartz (15 and 7%); micritic pellets (7 and 3%); and traces of feldspar. The matrix is composed of micrite and sparite (together totaling 40 and 43%, respectively, of the two samples), clays (mainly illite and chlorite, together totaling 10 and 1%, respectively, of the two samples), mica (0.5%), pyrite (1 and 2%), and plant material (2 and 4%). Both samples also show extensive hematite and limonite staining. A third sample from this lithology (59-1, 74–76 cm) contains considerably more clay (41%) and bioclastic debris (50%), and lesser amounts of quartz (7%), pyrite (1%), feldspar, and opaque minerals.

In contrast, three samples from the gray calcareous mudstone lithology (54-3, 128–131 cm, 55-4, 121–124 cm, and 56-3, 95–98 cm) (Fig. 2) are composed largely of micrite (70 and 87%), with lesser amounts of micritic pellets (0–15%); skeletal fragments (1 to 7%), which specifically include echinoderms (0.5–1.5%), brachiopods

[1] Graciansky, P. C. de, Poag, C. W., et al., *Init. Repts. DSDP*, 80: Washington (U.S. Govt. Printing Office).

[2] Address: (J. Mazzullo) Department of Geology, Texas A & M University, College Station, TX 77843; (E. K. Mazzullo, present address) Ocean Drilling Program, Texas A & M University; (K. Henke, present address) Exxon, Inc., Kingsville, TX.

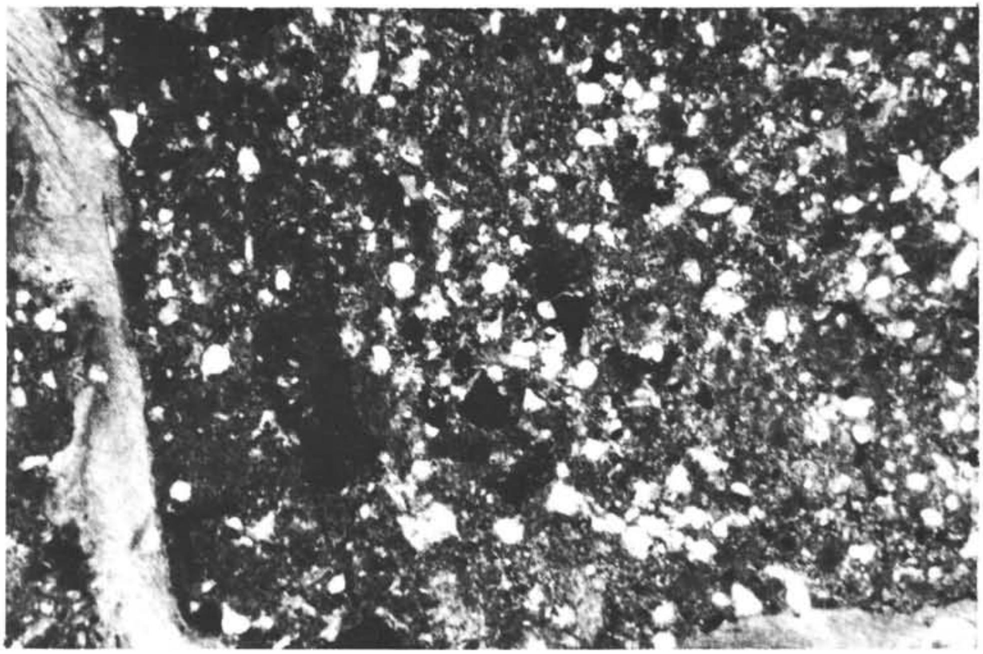

Figure 1. Sandy calcareous mudstone of Unit 8, Sample 60-1, 76–78 cm. Note the abundance of terrigenous and bioclastic sand debris. Crossed nicols, ×25.

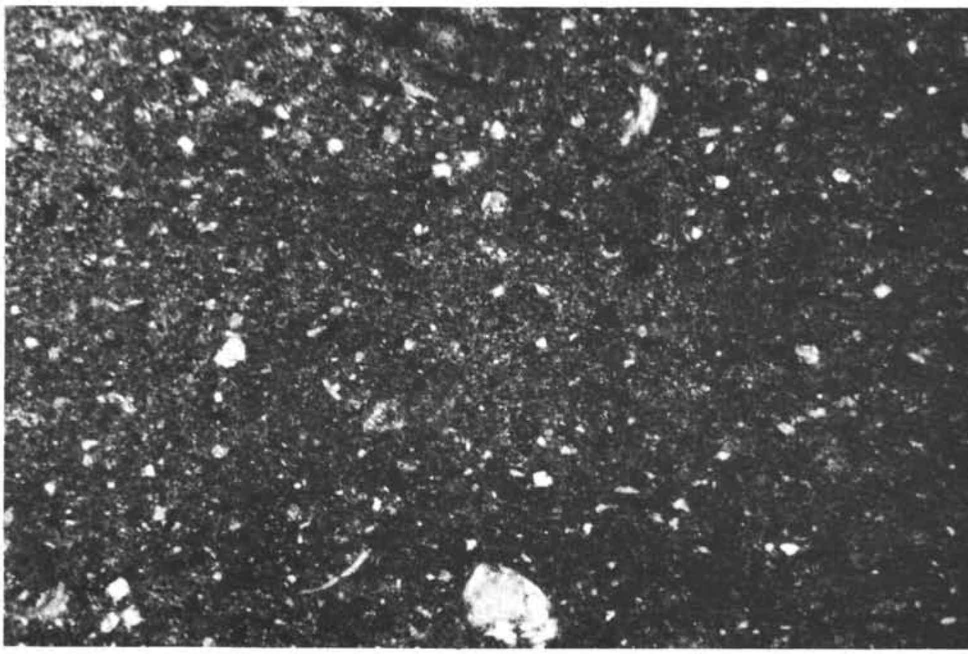

Figure 2. Calcareous mudstone of Unit 8, Sample 54-3, 128–131 cm. Crossed nicols, ×25.

(0.5–1.0%), foraminifers (0–3%), unidentifiable bioclasts (0.5–4%), and traces of bryozoans, pelecypods, algae, sponge spicules, and gastropods; as well as quartz (1.5–12%); clay (1–8%), which is largely illite, montmorillonite, and mixed-layer illite-montmorillonite; plant material (1%); and framboidal pyrite (1%). Patchy hematite stains were seen throughout the matrix and on pellets. Total mud content for these samples varies between 76 and 94%.

Lastly, two samples from the variegated calcareous mudstones at the top of the unit (Core 53) consist largely of hematite-stained micrite and clay (mostly illite). In Sample 53-1, 40–43 cm, the amounts of these two components were calculated as 16 and 51%, respectively; in Sample 53-2, 64–67 cm, they were optically indistinguishable because of unusually heavy hematite staining, but together totaled 70%. The remainder of this lithology consists of hematite-stained skeletal debris (0–3%), micritic pellets (0–15%), and quartz (4–15%). The total amount of mud in both samples varies between 78 and 82%. In Sample 53-2, 64–67 cm, sand-sized dolomite rhombohedrons (Fig. 3) recrystallized from the carbonate mud were abundant (26%).

Unit 9

Recovery from this unit (755–801.5 m BSF) was extremely poor, owing to the brittle nature of the sediment, and hence no samples were available for post-cruise study. The few samples available for study on board ship are described in the Site 549 chapter (this volume). Basically, this unit consists of carbonate grainstones and lesser amounts of algal mudstones.

Unit 10, Subunit a

Subunit 10a (801.5–843 m BSF) was described on board ship as gray calcareous sandy mudstones and wackestone interbedded with noncalcareous mudstones and sandy mudstones.

A thin section of the carbonate wackestone lithology (74-3, 75–78 cm) (Fig. 4), which predominates in Core

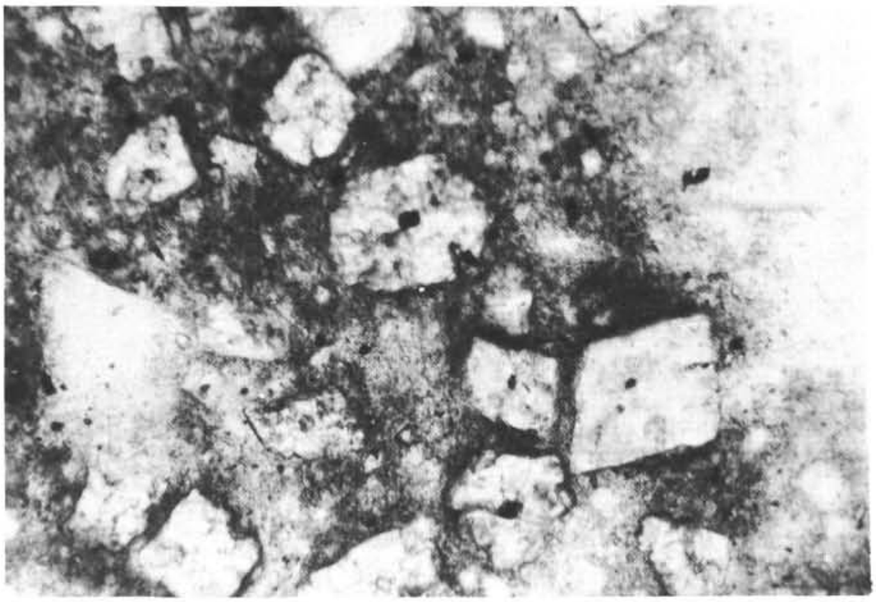

Figure 3. Authigenic dolomite rhombohedrons in Sample 53-2, 64–67 cm. Note also the dark hematite stain in the mud surrounding the dolomite. Plane light, ×120.

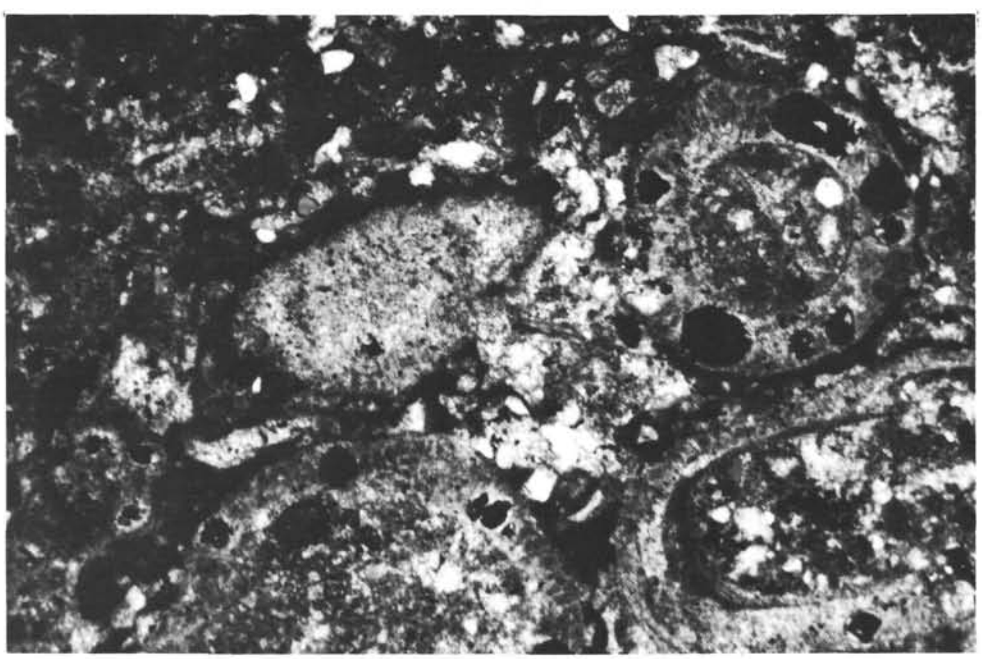

Figure 4. Carbonate wackestone in Subunit 10a, Sample 74-3, 75–78 cm. Note abundance of shell debris supported in a sparry matrix. Crossed nicols, ×120.

72 and is found periodically throughout Cores 74 to 77, showed it to consist of coarse sand- to gravel-sized shell debris (16%), small amounts of micritized pellets (3%), quartz (5%), pyrite (0.5%), and plant material (6.5%), all supported by a sparry calcite cement (62%), some of which presumably recrystallized from skeletal debris and mud. The identifiable shell debris consists of mollusc shells (10%) and lesser amounts foraminifers (2%), echinoderms (2%), cephalopods (1%), gastropods (0.5%), and brachiopods (0.5%). The muddier carbonate lithology (Sample 549-72,CC) is composed largely of micrite (90%) and minor amounts of quartz (8.4%), bioclasts (<1%), and framboidal pyrite (<1%).

The noncalcareous sandy mudstone (76-1, 61–64 cm) (Fig. 5) has a mud matrix composed of clay (69%) and micrite (3%); SEM and X-ray analyses indicate that the clay fraction consists largely of kaolinite and illite and minor amounts of chlorite. The sand fraction consists of quartz (18%), mica (3%), feldspar (1%), plant material (<1%), unknown bioclasts (1%), micritic pellets (3%), and pyrite (<1%). The rock as a whole is irregularly stained throughout with hematite. Lastly, the noncalcareous mudstone lithology (75-4, 25–28 cm) (Fig. 6) is composed mainly of clay (96%, mainly kaolinite, illite, and mixed-layer clays), and small amounts of sand-sized quartz (2%), muscovite (1%), and plant material (1%). Fossil debris is absent in this lithology.

Unit 10, Subunit b

Subunit 10b (843–870 m BSF) was described as consisting of massive, gray, calcareous sandstones and noncalcareous mudstones and sandy mudstones.

A thin section from the calcareous sandstone lithology (78-1, 92–94 cm) (Fig. 7) shows this lithology to be fairly silt rich (45%): thus, a more exact name for this lithology would be calcareous silty sandstone. The sand and silt fraction consists largely of quartz (39%), hematite- and limonite-stained micritic pellets (7%), echinoderms (2%), and other unidentifiable skeletal debris (2%). Clays, particularly kaolinite and illite, make up 6% of the sample. The sediment is cemented with sparite (43%) and lesser amounts of hematite (0.5%) and chalcedony (0.5%).

A sample of the noncalcareous mudstone lithology (79-1, 53–55 cm) was composed almost entirely of kaolinite, illite, and chlorite (94%), with minor amounts of quartz sand (5%) and carbonate skeletal clasts (1%).

Unit 10, Subunit c

Subunit 10c (870–884 m BSF) was described on board as consisting of variegated noncalcareous mudstones or sandy mudstones, and more rarely calcareous mudstones or sandy mudstones. Analysis of a sample (81-2, 31–32 cm) of the noncalcareous lithology indicates that it consists largely of kaolinite and illite (83%), with lesser amounts of sand-sized quartz (12%), pyrite (5%), and traces of plant debris and calcite spar.

Unit 10, Subunit d

Subunit 10d (884–964.5 m BSF) was described as thin interbeds of claystone, siltstone, mudstone, sandy mudstone, and sandstone, with an occasional thin layer of shelly limestone.

Two samples from the mudstone lithology (88-3, 64–67 cm and 89-1, 125–128 cm) (Fig. 8) contain large amounts of a kaolinite- and illite-dominated matrix (90 and 92%, respectively), and small amounts (9 and 7%) of sand- and silt-sized sediment, mostly quartz (5 and 3%), mica (1 and 2%), bioclasts (<1%), and pellets (<2%). Micrite was found in trace (0.5%) amounts in

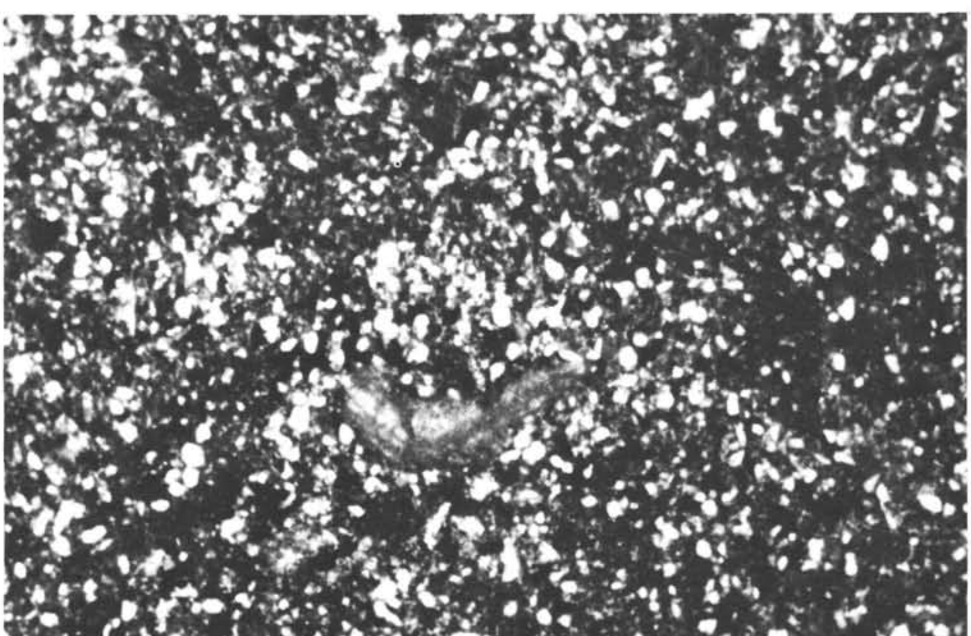

Figure 5. Noncalcareous sandy mudstone in Subunit 10a, Sample 76-1, 61–64 cm. Note abundance of sand-sized terrigenous debris (largely quartz). Crossed nicols, ×25.

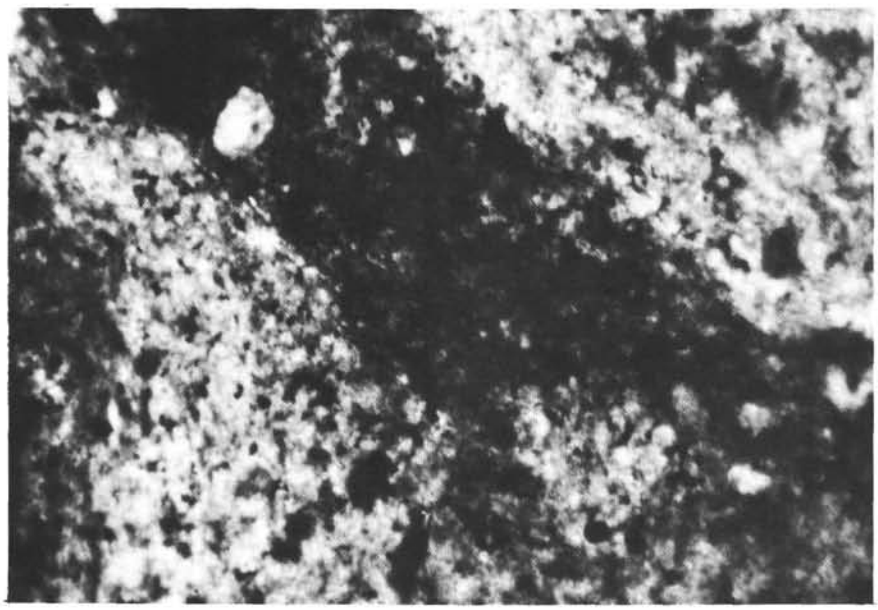

Figure 6. Noncalcareous mudstone lithology in Subunit 10a, Sample 75-4, 25-28 cm. Note abundance of clay and dark hematite stain. Crossed nicols, ×120.

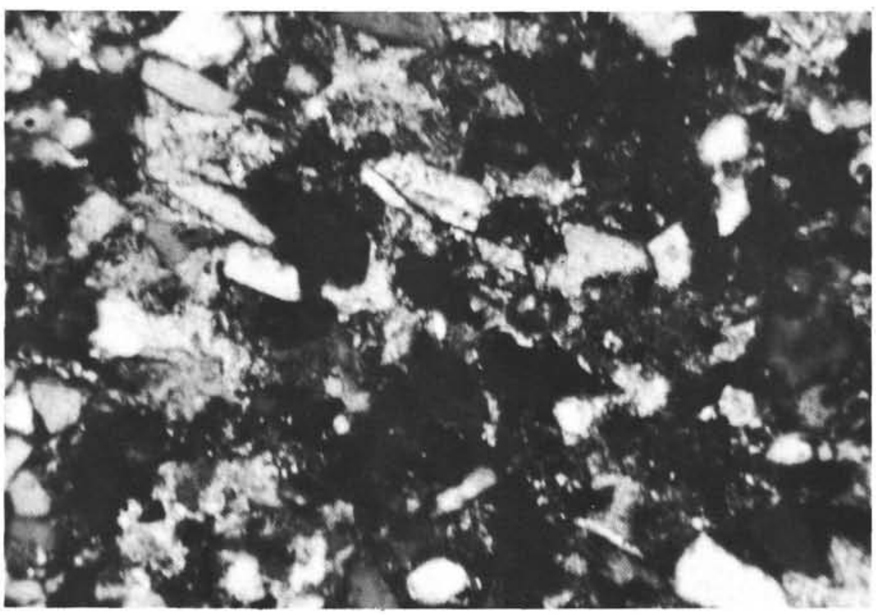

Figure 7. Calcareous silty sandstone of Subunit 10b, Sample 78-1, 92-94 cm. Note abundant silt-sized quartz and sparry cement. Crossed nicols, ×120.

Sample 89-1, 125-128 cm, and chlorite was found in minor amounts in Sample 88-3, 64-67 cm.

Three samples from the sandy mudstone lithology (86-2, 43-46 cm, 90-3, 3-6 cm, and 93-1, 41-43 cm) (Fig. 9) contained 21 to 25% sand- and silt-sized material, mostly quartz (13-15%), feldspar (0-4%), micritized pellets (0-4%), unidentifiable shell fragments (0-1%), plant material (2-4.5%), and pyrite (0-4%). The matrix consists largely of kaolinite and illite, with only trace amounts of micrite. Sample 86-2, 43-46 cm was originally described as a "mudstone," and 93-1, 41-43 cm was described as a "sandstone." However, both are clearly "sandy mudstones."

A sample from the "shelly limestone" lithology (88-4, 0-3 cm) (Fig. 10) is more properly described as a marly limestone or muddy wackestone. It contains 25.5% fossil fragments (mostly bivalve fragments) supported in an iron-stained, micritic and clay matrix that makes up 70% of the rock. Quartz sand and silt make up an additional 2% of this lithology. Another sample of this same

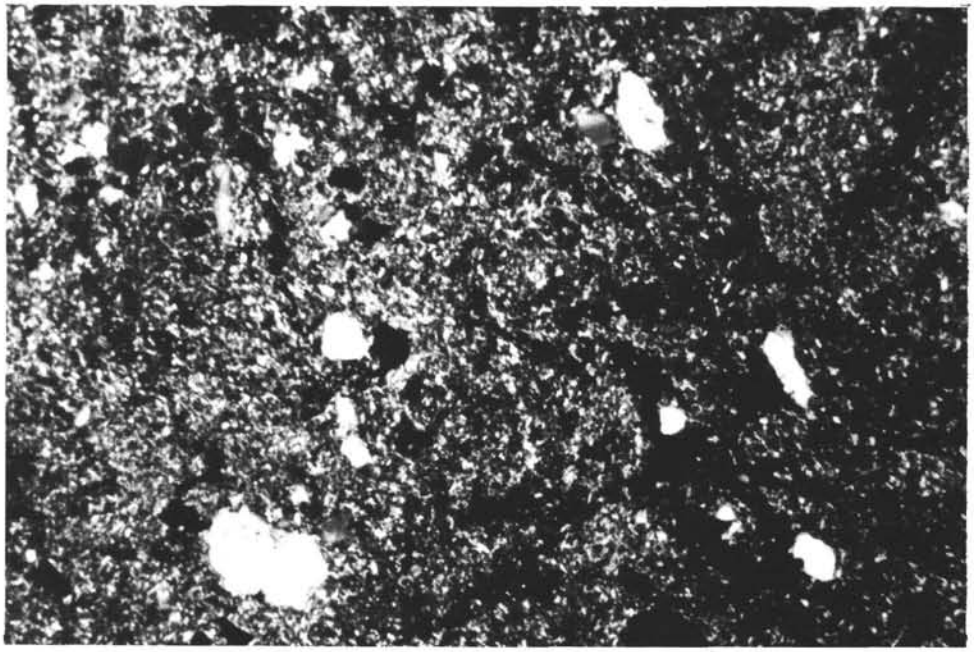

Figure 8. Mudstone in Subunit 10d, Sample 88-3, 64–67 cm. Note abundance of clay and small amount of quartz. Crossed nicols, ×25.

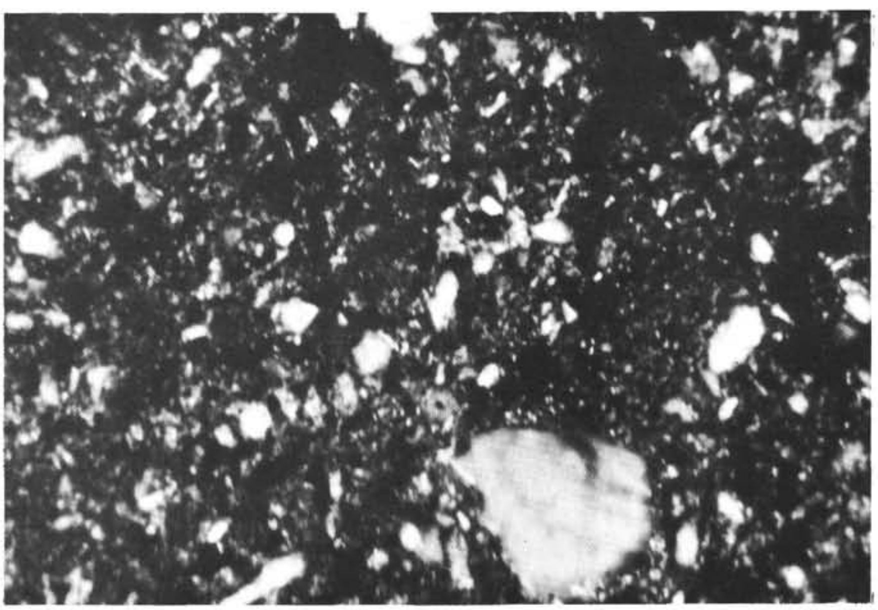

Figure 9. Sandy mudstone from Subunit 10d, Sample 90-3, 3–6 cm. Note the abundance of sand- and silt-sized quartz and the clayey matrix. Crossed nicols, ×120.

lithology (85-2, 45–48 cm) described on board as a siltstone is also a marly wackestone. This sample contains large shell fragments (15%), pellets (3%), quartz (23%), and plant material (4.5%), all supported in a matrix of micrite (35%) and clay (10%, largely kaolinite and illite). Framboidal pyrite is also very abundant in this sample (7.5%) (Fig. 11).

During sampling of this section on board ship for this study, samples of lithologies described as siltstone, claystone, and sandstone were deliberately chosen. Thin-section examination, however, showed such samples to be misnamed; most often these lithologies are more properly mudstones or sandy mudstones.

Similarly, one lithology not noted in the core descriptions is a calcareous sandy mudstone, represented by Sample 88-3, 0–3 cm (Fig. 12). This sample consists of a matrix of kaolinite and illite (56%) and micrite (8%) supporting sand-sized quartz (16%), fossil fragments (12%),

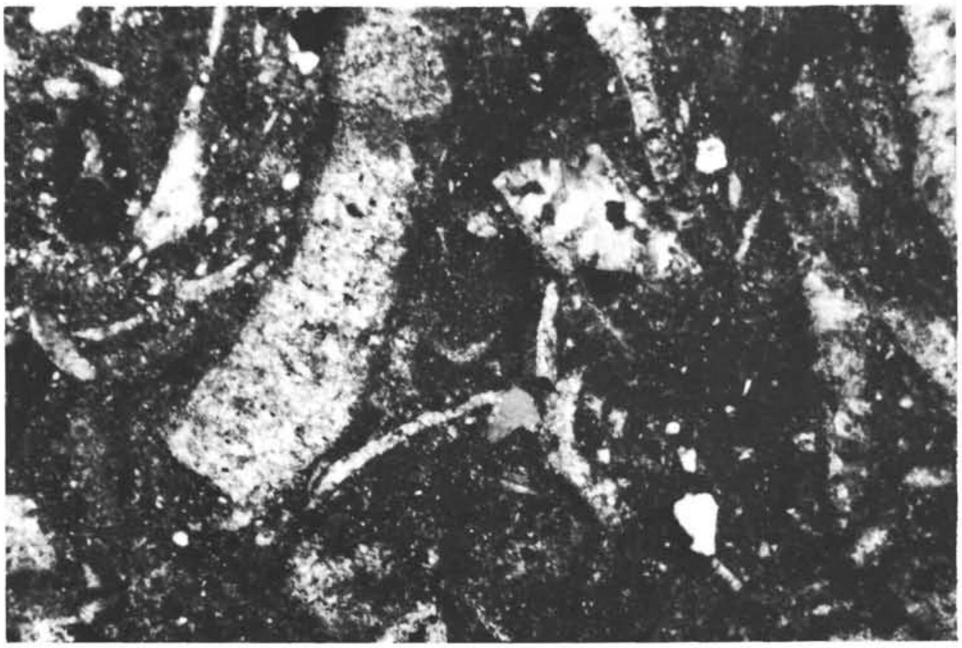

Figure 10. Wackestone in Subunit 10d, Sample 88-4, 0–3 cm. Note abundant shell debris supported in an iron-stained matrix of micrite and clay. Crossed nicols, ×25.

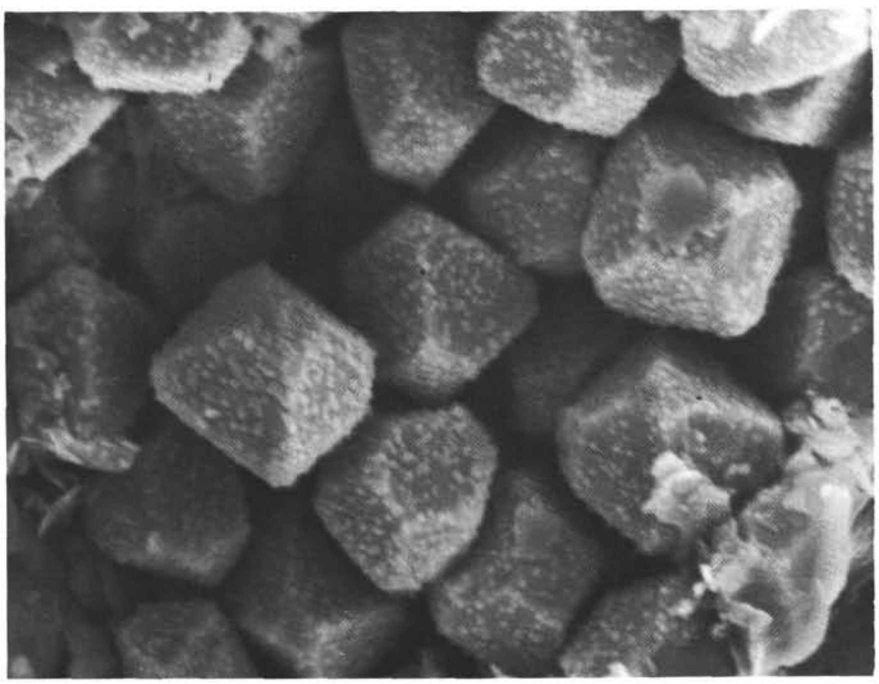

Figure 11. SEM imagery of framboidal pyrite, Sample 85-2, 45–48 cm; ×3000.

pellets (5%), plant material (2%), and pyrite (1%). This sample had previously been described as a sandy mudstone.

NOTES ON CLAY MINERALOGY

Mineralogic identification of clays was based on X-ray analyses, thin-section petrography, and SEM imagery. Each sample was analyzed by X-ray diffraction in four successive stages to determine the clay suite present: untreated, glycolated, heated to 400°C, and lastly, heated to 500°C (Carroll, 1978). No attempts were made to quantify the X-ray diffraction data in order to determine the relative proportion of all the clay minerals present. Rather, after X-ray diffraction, each sample was examined either in thin section or with the SEM, and only the clays present in the sample in major amounts were reported. Therefore, all references to changes are strictly qualitative and should be so construed. Lastly, the mor-

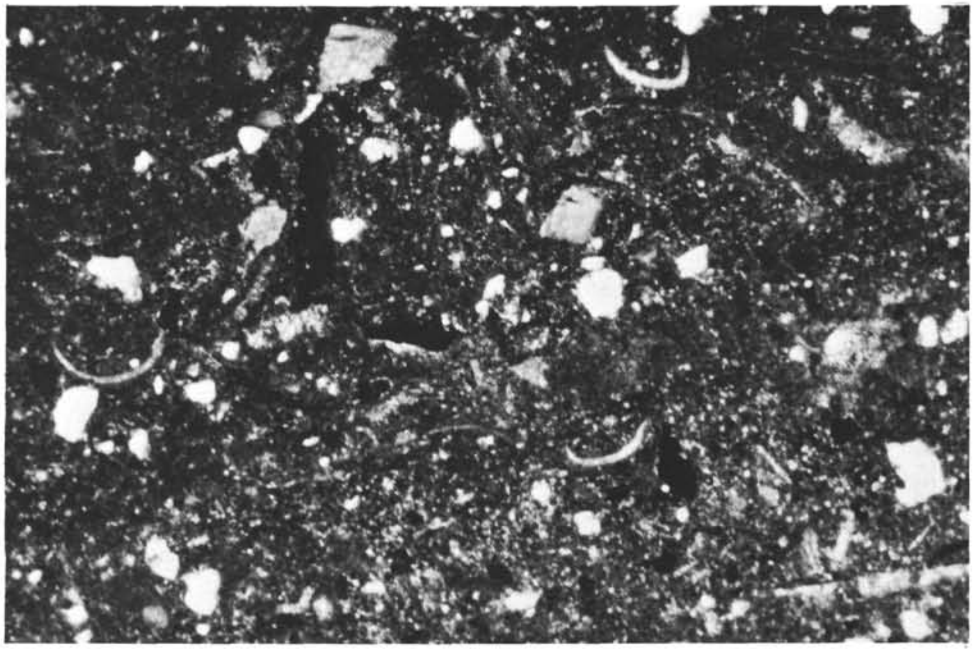

Figure 12. Calcareous sandy mudstone in Subunit 10d, Sample 88-3, 0–3 cm. Note abundance of sand-sized quartz and shell debris supported in a matrix dominated by clay. This sample was described on board ship as a sandy mudstone. Crossed nicols, ×25.

phology and location of the clays in each sample were examined with the SEM to determine whether they were detrital, authigenic, or recrystallized.

The clay suite in the synrift sediments is very diverse, with nearly every major clay group present in variable amounts. Two significant trends in clay mineral abundances, however, have been noted. The first is the presence of large amounts of kaolinite in Cores 74 through 93 and its absence in Cores above 74. (Kaolinite is considered to be the dominant clay mineral in fluvial, deltaic, and nearshore sediments [Weaver, 1958].) The second is the presence of large amounts of montmorillonite in Cores 53 through 74 and its absence in significant amounts below Core 74. (Montmorillonite is considered to be the dominant clay mineral in open-marine sediments.) SEM data indicate that most of the clays in the synrift sediments are detrital in origin, which is evidenced by the clays' usual occurrence as intercalated laminae, deformed by mechanical compaction (Fig. 13), or as dispersed matrix, sometimes grain supporting. Some of the clays, however, particularly kaolinite and to a lesser degree illite, have undergone recrystallization after deposition, as indicated by their well-developed morphology (Fig. 14) (Wilson and Pittman, 1977).

NOTES ON SMEAR SLIDES

One of the purposes of this study was to weight the advantages and disadvantages of the smear-slide technique used on board ship to describe the texture and composition of sediments. With this in mind, we have compared smear-slide descriptions of lithologic units as reported in the site chapter (this volume) with our thin-section data, and the conclusions we have reached are as follows.

First, we note that grain size estimates from smear slides are most accurate with fine-grained, well-sorted sediment of any composition and decrease in accuracy as grain size increases and degree of sorting lessens. The main reason for the discrepancy with more poorly sorted, sandy sediments lies in the preparation of the smear slide itself. During the application of the sample to the cover glass, coarser grains are segregated to the edges of the slide while muds occupy the center. This introduces a bias into the visual estimate of grain size, inasmuch as this technique assumes an even distribution of all components over the entire slide.

Second, the construction of a smear slide is a destructive process. Bioclasts and other fragile components, particularly cements, are destroyed by the process; also, grain-to-matrix relationships, such as occur in wackestones, are not evident in smear slides. This problem becomes most acute when dealing with coarser grained carbonate sedimentary rocks and precludes the use of Dunham and related classification schemes for such rocks.

Third, although composition is relatively easy to determine for silt- and clay-sized clasts, it is more difficult if grains are coarser, thicker, and more opaque. This is the most common problem with the sand-sized fraction of any sample, whether clastic or carbonate.

Lastly, there is a bias in the classification scheme for sediments in favor of fine-grained, siliceous and calcareous, biogenic sediments and against coarse clastics and carbonates. Chalks and oozes, for example, are very precisely categorized, whereas such diverse rocks as wackestones, grainstones, and boundstones are all lumped together into one general category "limestone". A more informative and detailed classification scheme for limestones is obviously needed.

Despite these drawbacks, the smear-slide technique worked relatively well with the rocks cored during Leg 80. The correlation between smear-slide and thin-section

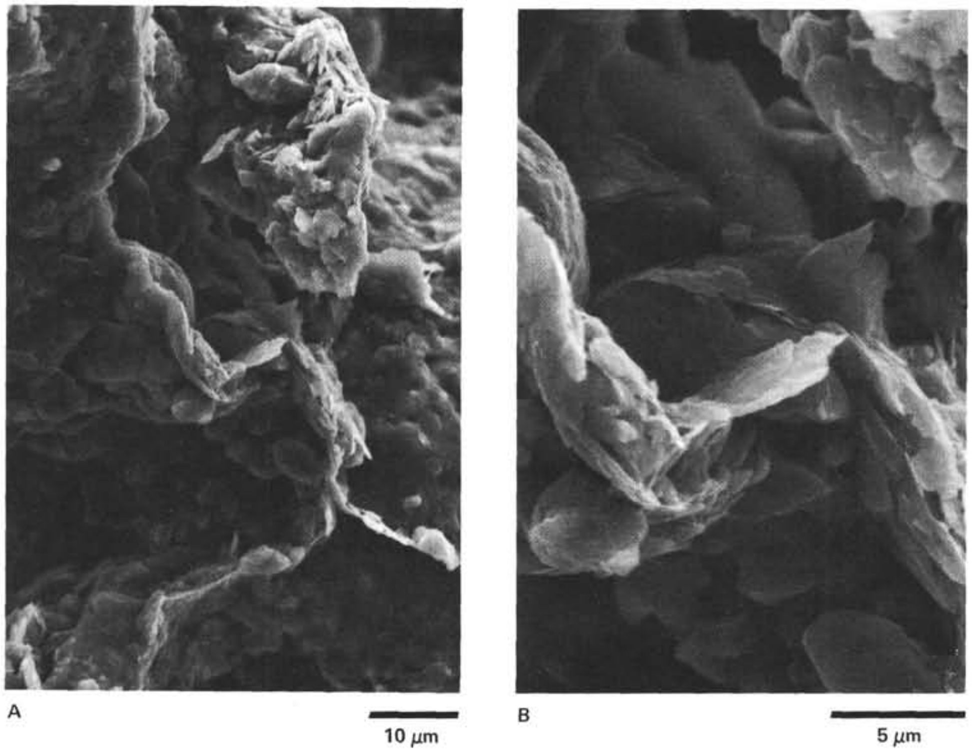

Figure 13. A. SEM imagery of clays in Sample 89-1, 125–128 cm, showing their occurrence as intercalated laminae of detrital origin subsequently deformed by postdepositional compaction. B. Close-up of same sample showing the well-developed morphology of the clays. Dispersive analysis of the clays identifies them as illite.

descriptions in our postcruise study of the sediments is generally good. The relative proportions of components estimated from smear slides are often in error by at least 10%, causing error in classification of the sample, but for most of the lithologies encountered during Leg 80, smear slides resulted in good descriptions, albeit semiquantitative and general, of samples in a short amount of time. The bulk of our stratigraphic section consisted of homogeneous, fine-grained lithologies, and we did not often encounter coarse lithologies, but even when we did, the comparison between smear-slide and thin-section data is favorable. We do recommend that for coarser sediments, the operator give more care to sample preparation so as to avoid any biasing of grain-size estimates, and he or she should use reflected light or a binocular microscope to identify the sandy components of the rock.

CONCLUSION: DEPOSITION OF UNITS 8 TO 10

On the basis of our textural and compositional analyses of samples from Units 8 and 10 and shipboard descriptions of samples from Unit 9, we conclude that the deposition of these units most likely occurred in shallow, semirestricted to open-marine environments during a marine transgression.

The basal Unit 10 was apparently deposited in very shallow nearshore waters. The presence of large amounts of mud, pyrite, and organic debris suggests rapid deposition in fairly low-energy, semirestricted waters of a lagoon, bay, or protected shelf rather than an open-marine shelf subjected to wave and tidal reworking. Clastic sediments in Unit 10 were presumably supplied from coastal deltaic sources, as indicated by their textural and compositional immaturity and the presence of abundant kaolinite (Weaver, 1958). The source of the carbonate mud, as always, is a controversial topic; opinions on the subject vary from *in situ* production by algae (Stockman et al., 1967) to abrasion of sand-sized clasts at a shelf margin and subsequent transport into a lagoon or bay (Bathurst, 1972; Pettijohn, 1975). Because of the amount of terrigenous mud in the section, it appears that conditions were not optimal for *in situ* production of all the carbonate mud in this unit. Rather, much of it was likely created by abrasion and then transported in from shelf margin facies (represented by Unit 9) by wave and storm washover.

Within Unit 10, the lowermost subunit (10d) was deposited in a distal deltaic environment proximal to a carbonate mud–rich zone. Distal deltaic sedimentation would have led to the deposition of the noncalcareous mudstone and sandy mudstone beds. Occasional storm washovers in turn would have deposited biogenic debris to produce the marly wackestone and calcareous sandy mudstone beds found in this subunit. Subunit 10c, which is composed largely of terrigenous and organic debris and pyrite and rare beds of calcareous sediments, was probably deposited in a similar, although somewhat more restricted or landward, environment than was Subunit 10d. In Subunit 10b, coarser carbonate lithologies are regularly interbedded with noncalcareous mudstones. De-

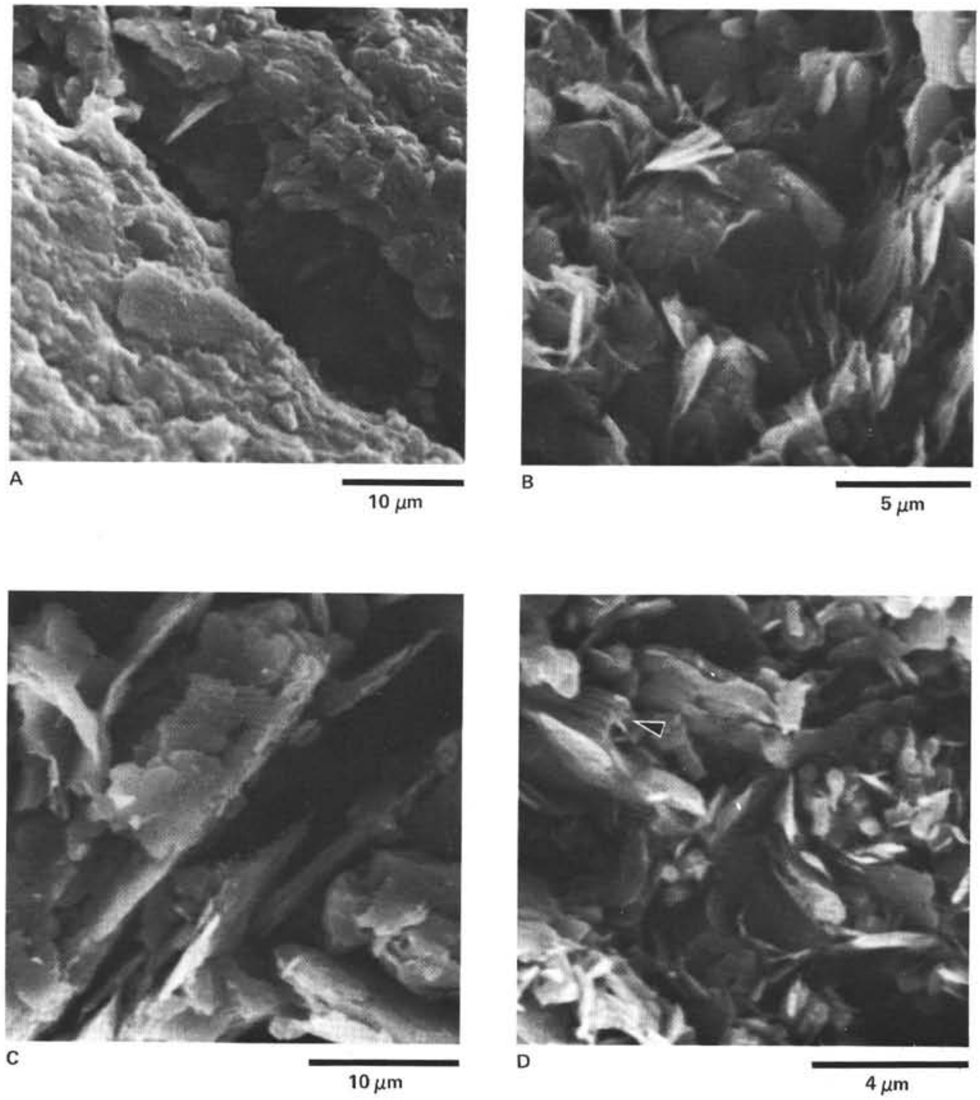

Figure 14. SEM imagery of recrystallized and detrital clays. A. Detrital illite coating sand grain in Sample 54-3, 128–131 cm. B. Same sample showing development of feathery illite recrystallized from the detrital illite. Clay identified by dispersive analysis. C. Recrystallized illite from Sample 89-1, 125–128 cm. D. Recrystallized kaolinite (arrow) and chlorite (in background) in Sample 79-1, 53–55 cm.

position of this subunit occurred farther seaward than either of the lower subunits, closer to the source of carbonate debris (the shelf margin). Lastly, Subunit 10a, which contains more, particularly coarse-grained, carbonate debris and less terrigenous mud than any lower subunit, was probably deposited closest to the shelf margin and farthest from the clastic-dominated shoreline.

On the basis of onboard descriptions, Unit 9 was probably deposited as milliporoid boundstones and skeletal grainstones at a high-energy, well-oxygenated shelf margin. These carbonate sediments presumably formed a bank that absorbed wave, tidal, and storm energy and protected the more landward environments (represented by Unit 10) from these high-energy sources.

Unit 8 represents the final phase of marine transgression. A combination of increased water depth, landward shoreline migration, and the presence of a carbonate bank resulted in a sharp decrease in clastic sediment influx and the deposition of carbonate wackestones and mudstones seaward of the shelf margin. The upward gradation from highly fossiliferous wackestones to nonfossiliferous, fine-grained micritic mudstones in this unit suggests deposition in progressively deeper and less productive foreslope environments, where most of the sediment was derived from downslope movement of shelf margin debris.

ACKNOWLEDGMENTS

The authors wish to thank the Department of Geology, Texas A & M University and the Mini-Grant Committee of Texas A & M University for their financial support for this project. We also wish to thank R. J. Stanton and T. T. Tieh for their constructive comments.

REFERENCES

Bathurst, R. G. C., 1972. *Carbonate Sediments and Their Diagenesis:* New York (American Elsevier).

Carroll, D., 1978. Clay minerals: a guide to their X-ray identification. *Spec. Pap. Geol. Soc. Am.,* 126.

Pettijohn, F. J., 1975. *Sedimentary Rocks:* New York (Harper and Row).

Stockman, K. W., Ginsburg, R. N., and Shinn, E. A., 1967. The production of lime mud by algae in south Florida. *J. Sed. Pet.,* 37: 633–648.

Weaver, C. E., 1958. Geologic interpretation of argillaceous sediments. *Am. Assoc. Pet. Geol. Bull.,* 42:254–309.

Wilson, M. D., and Pittman, E. D., 1977. Authigenic clays in sandstones: Recognition and influence on reservoir properties and paleoenvironmental analysis. *J. Sed. Pet.,* 47:3–31.

Date of Initial Receipt: December 6, 1982
Date of Acceptance: July 18, 1983